Early Myocardial Infarction Detection with One-Class Classification over Multi-view Echocardiography

Aysen Degerli[†], Fahad Sohrab[†], Serkan Kiranyaz[*], Moncef Gabbouj[†]

[†]Tampere University, Tampere, Finland
[*]Qatar University, Doha, Qatar

Abstract

Myocardial infarction (MI) is the leading cause of mortality and morbidity in the world. Early therapeutics of MI can ensure the prevention of further myocardial necrosis. Echocardiography is the fundamental imaging technique that can reveal the earliest sign of MI. However, the scarcity of echocardiographic datasets for the MI detection is the major issue for training data-driven classification algorithms. In this study, we propose a framework for early detection of MI over multi-view echocardiography that leverages one-class classification (OCC) techniques. The OCC techniques are used to train a model for detecting a specific target class using instances from that particular category only. We investigated the usage of uni-modal and multi-modal one-class classification techniques in the proposed framework using the HMC-QU dataset that includes apical 4-chamber (A4C) and apical 2-chamber (A2C) views in a total of 260 echocardiography recordings. Experimental results show that the multi-modal approach achieves a sensitivity level of 85.23% and F1-Score of 80.21%.

1. Introduction

World Health Organization (WHO) has recently reported that coronary artery disease (CAD) is the reason for 16% of total deaths worldwide [1]. Myocardial infarction (MI) is the most severe manifestation of CAD that leads to irreversible necrosis of the myocardium [2]. Hence, early diagnosis of MI plays a vital role in the prevention of mortality and morbidity. Accordingly, the presentation of MI is recognized by its symptoms and several clinical features that are the biochemical markers, electrocardiography (ECG) findings, and imaging techniques [3]. However, the symptoms of MI, i.e., shortness of breath and pain around the upper body, may not be visible in the early stages [4]. Furthermore, the biochemical values of myocardial necrosis, such as the high sensitivity cardiac troponin (hs-cTn), take time to evolve to a diagnostic level for MI [5, 6]. On the other hand, the changes at the ECG are occasionally non-diagnostic and also have a significant delay compared to imaging techniques [6]. Echocardiography is a non-invasive imaging technique that reveals the earliest sign of MI, which is the regional wall motion abnormality (RWMA) of the necrosed myocardium [7]. Hence, echocardiography has the potential to be the most useful diagnostic tool to detect early MI with easy accessibility and low-cost options [8].

The diagnosis of MI using echocardiography has several drawbacks, where the RWMA assessment is highly subjective, and the recordings generally have low image quality with a high level of noise [7, 9]. Thus, computer-aided diagnosis algorithms have become a necessity for MI detection. However, many studies [10–13] have evaluated their algorithms over scarce, private, synthetic, and single-view echocardiographic data which causes certain reliability and robustness issues, especially for deep learning models. Contrary to class-specific algorithms, one-class classification (OCC) models require only the positive class during training with much fewer samples [14, 15]. However, despite their feasibility, only the studies [16, 17] have used OCC models for echocardiographic data.

In this study, we propose a framework that leverages OCC for the early detection of MI using multi-view echocardiography as depicted in Figure 1. First, we extract features from apical 4-chamber (A4C), and apical 2-chamber (A2C) view echocardiography recordings by tracking the motion of the left ventricle (LV) using Active Polynomials (APs) [18]. Then, we use a multi-modal OCC approach over the maximum displacement features of A4C and A2C views. As the pioneer study with multi-modal OCC for the MI diagnosis using multi-view echocardiography, we have extensively evaluated both multi-, and uni-modal OCC algorithms over the HMC-QU[1] dataset.

The paper proceeds as follows. In Section 2, we propose the framework for early MI detection. In Section 3, we report the experimental results and conclude the paper in Section 4.

[1]The benchmark HMC-QU dataset is publicly shared at the repository https://www.kaggle.com/aysendegerli/hmcqu-dataset

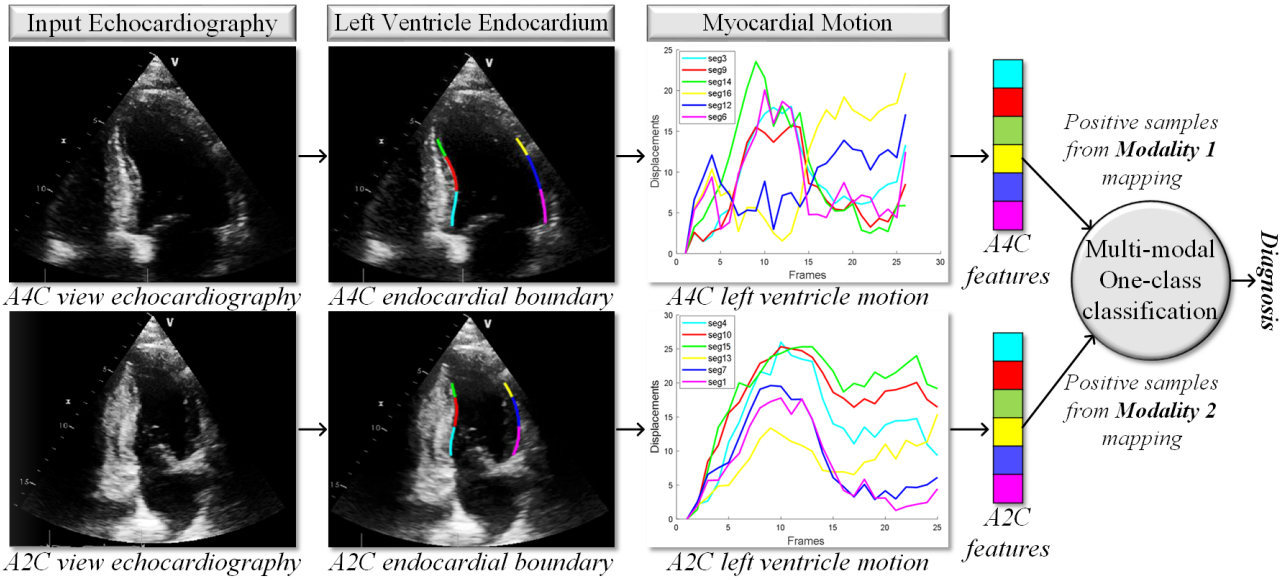

Figure 1: The proposed framework for early detection of MI with multi-modal one-class classification over multi-view echocardiography, where the features of both modalities are mapped to a shared subspace to perform diagnosis.

2. Methodology

The accurate extraction of the LV endocardium is a crucial step in myocardial motion tracking. In this study, the endocardial boundary of the LV from A4C and A2C views are extracted by Active Polynomials (APs) [19] that are the constrained versions of active contours [20]. In order to overcome the common issues due to the low-quality in echocardiography, APs are formed by encapsulating the LV by a thick wall around the chamber, and then, the active contour is initialized and evolved towards the endocardium. Once the APs are formed over each frame of echocardiography recordings, the LV wall is divided into a total of 12 distinct myocardial segments. Thus, myocardial motion is obtained for each myocardial segment as depicted in Figure 1.

The feature engineering is performed as in our previous study [18], where we extract the feature vectors from A4C (modality 1) and A2C (modality 2) view echocardiography recordings in one-cardiac cycle. In the proposed framework, we used OCC for training the predictive model. Contrary to class-specific algorithms, the OCC models do not require information from negative samples during training. For the OCC model, we propose using the Multi-modal Subspace Support Vector Data Description (MS-SVDD) [21] due to its feasibility with multi-view echocardiographic data. MS-SVDD maps the multi-view feature vectors to a lower-dimensional optimized feature space shared by features from different views of echocardiography as illustrated in Figure 1. The feature vectors of view v are represented by $\mathbf{F}_v = [f_{v,1}, f_{v,2}, ..., f_{v,6}]$, $\mathbf{f}_{v,i} \in \mathbb{R}^{D_v}$, where the dimensionality of the original feature space is D_v. Accordingly, a projection matrix $\mathbf{Q}_v \in \mathbb{R}^{d \times D_v}$ is formed for each modality v that projects the feature vectors $\mathbf{F}_v$ into a lower $d-$dimensional shared subspace optimized for OCC. Hence, MS-SVDD is trained by the target data that fits into the smallest hypersphere by minimizing the following function:

$$\begin{aligned} \min F(R, \mathbf{a}) &= R^2 + C \sum_{v=1}^{V} \sum_{i=1}^{N} \xi_{v,i} \\ \text{s.t. } ||\mathbf{Q}_v \mathbf{f}_{v,i} - \mathbf{a}||_2^2 &\leq R^2 + \xi_{v,i}, \xi_{v,i} \geq 0, \\ \forall v \in \{1, \ldots, V\}, &\forall i \in \{1, \ldots, N\}, \end{aligned} \tag{1}$$

where R is the radius, $\mathbf{a}$ is the center of hypersphere, $\xi_{v,i}$ are slack variables, and C controls the outliers in the training set. Then, $\mathbf{Q}_v$ is updated as $\mathbf{Q}_v \leftarrow \mathbf{Q}_v - \eta \Delta L$, where ΔL is the gradient of Lagrangian of Eq. (1) for the corresponding modality v, and η is the learning rate. Different regularization techniques (r) are also used in MS-SVDD by considering the co-variance of data from different modalities in the shared subspace. The regularization term expressing the co-variance of selected data is represented by ω and the importance of ω is controlled by a hyper-parameter β.

In this study, we also investigate the uni-modal OCC algorithms: One-class Support Vector Machine (OC-SVM) [22], Support Vector Data Description (SVDD) [23], Subspace SVDD (S-SVDD) [15], and Ellipsoidal Subspace SVDD (ES-SVDD) [24]. Contrary to MS-SVDD, where

Table 1: Average myocardial infarction detection performance results (%) computed over the test sets of each $5-$fold in HMC-QU dataset.

	Target: MI							Target: non-MI						
	r	Sen	Spe	Pre	F1	Acc	GM	r	Sen	Spe	Pre	F1	Acc	GM
Non-linear one-class classification														
MS-SVDD$_{ds_1}$	ω_1	70.45	61.90	**79.49**	74.70	67.69	**66.04**	ω_0	71.43	53.41	42.25	53.10	59.23	61.77
MS-SVDD$_{ds_2}$	ω_2	63.64	42.86	70.00	66.67	56.92	52.23	ω_0	61.90	73.86	53.06	57.14	70.00	67.62
MS-SVDD$_{ds_3}$	ω_2	55.68	59.52	74.24	63.64	56.92	57.57	ω_0	57.14	57.95	39.34	46.60	57.69	57.54
MS-SVDD$_{ds_4}$	ω_6	39.77	**76.19**	77.78	52.63	51.54	55.05	ω_2	73.81	67.05	51.67	**60.78**	69.23	**70.35**
ES-SVDD	ψ_0	73.86	38.10	71.43	72.63	62.31	53.05	ψ_0	69.05	56.82	43.28	53.21	60.77	62.64
S-SVDD	ψ_2	59.09	54.76	73.24	65.41	57.69	56.88	ψ_1	54.76	52.27	35.38	42.99	53.08	53.50
SVDD	–	80.68	38.10	73.20	76.76	66.92	55.44	–	69.05	71.59	53.70	60.42	**70.77**	70.31
OC-SVM	–	42.05	71.43	75.51	54.01	51.54	54.81	–	35.71	**82.95**	50.00	41.67	67.69	54.43
Linear one-class classification														
MS-SVDD$_{ds_1}$	ω_5	81.82	47.62	76.60	79.12	70.77	62.42	ω_2	73.81	62.50	48.44	58.49	66.15	67.92
MS-SVDD$_{ds_2}$	ω_2	54.55	59.52	73.85	62.75	56.15	56.98	ω_2	78.57	36.36	37.08	50.38	50.00	53.45
MS-SVDD$_{ds_3}$	ω_0	67.05	59.52	77.63	71.95	64.62	63.17	ω_5	73.81	50.00	41.33	52.99	57.69	60.75
MS-SVDD$_{ds_4}$	ω_5	85.23	42.86	75.76	**80.21**	**71.54**	60.44	ω_0	**80.95**	59.09	48.57	60.71	66.15	69.16
ES-SVDD	ψ_3	82.95	35.71	73.00	77.66	67.69	54.43	ψ_3	45.24	67.05	39.58	42.22	60.00	55.08
S-SVDD	ψ_3	70.45	45.24	72.94	71.68	62.31	56.45	ψ_2	50.00	70.45	44.68	47.19	63.85	59.35
SVDD	–	**86.36**	33.33	73.08	79.17	69.23	53.65	–	69.05	69.32	51.79	59.18	69.23	69.18
OC-SVM	–	44.32	73.81	78.00	56.52	53.85	57.19	–	47.62	81.82	**55.56**	51.28	**70.77**	62.42

the feature vectors are projected to a joint subspace suitable for OCC, in the uni-modal OCC methods, we concatenate the feature vectors of A4C and A2C views as $\mathbf{F} = \begin{bmatrix}\mathbf{F}_1 \, \mathbf{F}_2\end{bmatrix} \in \mathbb{R}^{(D_1+D_2)\times N}$. In uni-modal subspace OCC methods (S-SVDD, ES-SVDD), the corresponding regularization technique is denoted by ψ.

3. Experimental Evaluation

In this section, the experimental setup is introduced. Then, the experimental results are reported over the HMC-QU dataset.

3.1. Experimental Setup

The performance of the proposed framework is evaluated over the HMC-QU dataset [18] that includes a total of 260 echocardiography recordings from A4C and A2C views of 130 individuals with the ground-truths of 88 MI patients, and 42 non-MI subjects. During the training of the OCC models, we consider the target class as MI or non-MI, and report the results for both targets. Accordingly, noting that the target class is the positive class, we calculate the standard performance metrics as follows: Sensitivity (Sen) is the ratio of correctly detected positive samples in the positive class, Specificity (Spe) is the rate of accurately identified negative samples in the negative class, Precision (Pre) is the ratio of correctly detected target samples among the samples that are identified as the positive class, F1$-$Score (F1) is the harmonic mean of *Sen* and *Pre*, Accuracy (Acc) is the ratio of correctly classified samples over the dataset, and GMean (GM) is the geometric mean of *Sen* and *Spe*.

The OCC models are evaluated in a stratified $5-$fold cross-validation (CV) scheme with a ratio of 80% training to 20% test sets. The best hyper-parameters for the testing phase are determined by an exhaustive search over a stratified $10-$fold CV scheme with respect to the best GM during training. We have experimented with both linear and non-linear (kernel) versions of the OCC models, where we used the kernel $K_{i,j} = \exp\left(\frac{-||\mathbf{f}_i - \mathbf{f}_j||^2}{2\sigma^2}\right)$ with the hyper-parameter σ. The hyper-parameters η, β, C, σ, and d are searched as follows: $\eta \in \{10^{-4}, 10^{-3}, 10^{-2}, 10^{-1}, 1\}$, $\beta \in \{10^{-4}, 10^{-3}, 10^{-2}, 10^{-1}, 1, 10, 10^2, 10^3, 10^4\}$, $C \in \{0.01, 0.05, 0.1, 0.2, 0.3, 0.4, 0.5, 0.6\}$, $\sigma \in \{10^{-2}, 10^{-1}, 1, 10, 10^2, 10^3\}$, in multi-modal $d \in [1, 5]$, whereas in uni-modal $d \in [1, 11]$ with a gap of 1 increasing at each step. Moreover, the MS-SVDD has different decision strategies ds_1, ds_2, ds_3, ds_4, where the details are presented in [21]. Lastly, the implementation of the OCC models is performed on MATLAB R2020a.

3.2. Experimental Results

In this section, we investigate the performances of multi- and uni-modal OCC models for different targets with linear and non-linear versions. The performances are reported in Table 1. Primarily, the best GM of 66.04% and 70.35% are obtained by non-linear MS-SVDD for MI and non-MI targets, respectively. It can be observed that non-linear MS-SVDD$_{ds_1}$ has achieved the highest precision of 79.49% for target MI, where the decision strategy 1 is performed that merges the decisions of both modalities by

Table 2: Confusion matrices of the linear SVDD (a) and MS-SVDD$_{ds_4}$ (b) models with target MI.

(a)

SVDD		Predicted	
		Non-MI	MI
Ground Truth	Non-MI	14	28
	MI	12	76

(b)

MS-SVDD$_{ds_4}$		Predicted	
		Non-MI	MI
Ground Truth	Non-MI	18	24
	MI	13	75

the *AND* operator in the testing phase. Moreover, the best F1−Score of 80.21% is achieved by linear MS-SVDD$_{ds_4}$ for target MI with an elegant sensitivity level of 85.23%, where only the decision of the second modality is considered in the testing phase. The best sensitivity level of 86.36% is obtained by linear SVDD for target MI which is very close to the sensitivity of linear MS-SVDD$_{ds_4}$, where their confusion matrices are shown in Table 2.

4. Conclusions

The early diagnosis of MI is a crucial task to prevent the further myocardial necrosis. This study investigates the OCC algorithms for the first time for multi-view echocardiography. The experimental results over the HMC-QU dataset have revealed that multi-modal OCC models have achieved the highest precision of 79.49% and F1−Score of 80.21% despite the decent performance of the uni-modal OCC algorithms. Furthermore, we have investigated the linear and non-linear options of the presented OCC algorithms, and experimentally showed that the best GMean of 70.35% is achieved by the multi-modal OCC model.

Acknowledgments

This study was supported in part by the NSF-Business Finland Center for Visual and Decision Informatics (CVDI) Advanced Machine Learning for Industrial Applications (AMaLIA) under Grant 4183/31/2021, and in part by the Haltian Stroke-Data projects.

References

[1] World Health Organization (WHO). The top 10 causes of death, 2020. Available online: https://www.who.int/en/news-room/fact-sheets/detail/the-top-10-causes-of-death (accessed on 05 April 2022).

[2] Reed GW, Rossi JE, Cannon CP. Acute myocardial infarction. The Lancet 2017;389(10065):197–210.

[3] Thygesen K, Alpert JS, Jaffe AS, Simoons ML, Chaitman BR, White HD. Third universal definition of myocardial infarction. Circulation 2012;126(16):2020–2035.

[4] Thygesen K, Alpert JS, White HD. Universal definition of myocardial infarction. J Am Coll Cardiol 2007; 50(22):2173–2195.

[5] MacRae AR, Kavsak PA, Lustig V, Bhargava R, Vandersluis R, Palomaki GE, Yerna MJ, Jaffe AS. Assessing the requirement for the 6-hour interval between specimens in the american heart association classification of myocardial infarction in epidemiology and clinical research studies. Clin Chem 2006;52(5):812–818.

[6] Esmaeilzadeh M, Parsaee M, Maleki M. The role of echocardiography in coronary artery disease and acute myocardial infarction. J Tehran Heart Cent 2013;8(1):1–13.

[7] Porter TR, Mulvagh SL, Abdelmoneim SS, Becher H, Belcik JT, Bierig M, Choy J, Gaibazzi N, Gillam LD, Janardhanan R, et al. Clinical applications of ultrasonic enhancing agents in echocardiography: 2018 american society of echocardiography guidelines update. J Am Soc Echocardiogr 2018;31(3):241–274.

[8] Chatzizisis YS, Murthy VL, Solomon SD. Echocardiographic evaluation of coronary artery disease. Coron Artery Dis 2013;24(7):613–623.

[9] Degerli A, Zabihi M, Kiranyaz S, Hamid T, Mazhar R, Hamila R, Gabbouj M. Early detection of myocardial infarction in low-quality echocardiography. IEEE Access 2021;9:34442–34453.

[10] Suhling M, Arigovindan M, Jansen C, Hunziker P, Unser M. Myocardial motion analysis from b-mode echocardiograms. IEEE Trans Image Process 2005;14(4):525–536.

[11] Jamal F, Strotmann J, Weidemann F, Kukulski T, D'hooge J, Bijnens B, Van de Werf F, De Scheerder I, Sutherland GR. Noninvasive quantification of the contractile reserve of stunned myocardium by ultrasonic strain rate and strain. Circulation 2001;104(9):1059–1065.

[12] Chalana V, Linker D, Haynor D, Kim Y. A multiple active contour model for cardiac boundary detection on echocardiographic sequences. IEEE Trans Med Imaging 1996; 15(3):290–298.

[13] Omar HA, Patra A, Domingos JS, Leeson P, Noblel AJ. Automated myocardial wall motion classification using handcrafted features vs a deep cnn-based mapping. In Conf. Proc. IEEE Eng. Med. Biol. Soc. (EMBC). IEEE, 2018; 3140–3143.

[14] Sohrab F, Raitoharju J. Boosting rare benthic macroinvertebrates taxa identification with one-class classification. In IEEE Symp. Ser. Comput. Intell. (SSCI). 2020; 928–933.

[15] Sohrab F, Raitoharju J, Gabbouj M, Iosifidis A. Subspace support vector data description. In Int. Conf. Pattern Recognit (ICPR). IEEE, 2018; 722–727.

[16] Gong Y, Zhang Y, Zhu H, Lv J, Cheng Q, Zhang H, He Y, Wang S. Fetal congenital heart disease echocardiogram screening based on dgacnn: Adversarial one-class classification combined with video transfer learning. IEEE Trans Med Imaging 2020;39(4):1206–1222.

[17] Loh B, Fong A, Ong T, Then P. P203 unsupervised one-class classification and anomaly detection of stress echocardiograms with deep denoising spatio-temporal autoencoders. Eur Heart J 2020;41(Supplement_1):ehz872–074.

[18] Degerli A, Kiranyaz S, Hamid T, Mazhar R, Gabbouj M. Early myocardial infarction detection over multi-view echocardiography. arXiv preprint arXiv211105790 2021;.

[19] Kiranyaz S, Degerli A, Hamid T, Mazhar R, Fadil Ahmed RE, Abouhasera R, Zabihi M, Malik J, Hamila R, Gabbouj M. Left ventricular wall motion estimation by active polynomials for acute myocardial infarction detection. IEEE Access 2020;8:210301–210317.

[20] Kass M, Witkin A, Terzopoulos D. Snakes: Active contour models. Int J Comput Vision 1988;1(4):321–331.

[21] Sohrab F, Raitoharju J, Iosifidis A, Gabbouj M. Multimodal subspace support vector data description. Pattern Recognit 2021;110:107648.

[22] Schölkopf B, Williamson RC, Smola A, Shawe-Taylor J. Sv estimation of a distribution's support, 1999.

[23] Tax DM, Duin RP. Support vector data description. Mach Learn 2004;54(1):45–66.

[24] Sohrab F, Raitoharju J, Iosifidis A, Gabbouj M. Ellipsoidal subspace support vector data description. IEEE Access 2020;8:122013–122025.

Address for correspondence:

Aysen Degerli

P.O. Box 553, FI−33014, Tampere Finland

aysen.degerli@tuni.fi